UDC 539.4

Study of Characteristic Equation of the Elastic Stress Field near Bimaterial Notches

H. Arabi,[a,1] M. M. Mirsayar,[b] A. T. Samaei,[b] and M. Darandeh[a]

[a] Azad University of Garmsar, Garmsar, Iran

[b] Iran University of Science and Technology, Narmak, Tehran, Iran

[1] habibarabi1@yahoo.com

УДК 539.4

Анализ характеристического уравнения упругого поля напряжений вблизи надрезов на стыке двух материалов

Х. Араби[а], М. М. Мирсаяр[б], А. Т. Самаэй[б], М. Дарандех[а]

[а] Университет Азад Гермсар, Гермсар, Иран

[б] Иранский университет науки и технологии, Тегеран, Иран

Исследуется характеристическое уравнение для упругого поля напряжений у вершины надреза на стыке двух материалов. Установлено, что разрушение происходит в угловых точках их стыка из-за возникновения сингулярных напряжений вследствие разрыва сплошности материала и особенностей геометрической конфигурации. В поле упругих напряжений у вершины надреза на стыке двух материалов порядок такой сингулярности определяют собственные значения функции напряжений Эри. Выполнен анализ сингулярных собственных значений и малоизученного первого несингулярного собственного значения. Рассмотрены различные комбинации материалов и геометрических конфигураций для двух наиболее используемых траекторий на диаграмме Боги ($\beta = 0$, $\beta = \alpha/4$) и детально проанализированы полученные результаты. Показано, что геометрические конфигурации и комбинации материалов у вершины надреза существенно влияют на сингулярность напряжений вблизи угловых точек надреза. Области с высокой сингулярностью напряжений были выделены между линиями $\beta = 0$ и $\beta = \alpha/4$ на диаграмме Боги и проанализированы как для первого, так и второго сингулярного собственного значения.

Ключевые слова: надрез на стыке двух материалов, сингулярные собственные значения, первое несингулярное собственное значение, характеристическое уравнение, поле упругих напряжений.

Introduction. Today, bonded joints are used in manufacturing of many modern structures such as micromechanical devices, adhesively bonded joints and composite materials [1–6]. In structures containing these bonds, combination of materials and geometrical configuration are a critical source of stress singularity, and failure usually occurs at these corners.

In order to study the fracture mechanism of these bonds, a sufficient knowledge on the variation of eigenvalues extracted from characteristic equation of the elastic stress field is definitely one of the most important steps. These eigenvalues determine the order of singularity near the bimaterial notch tip. The characteristic

equation for a bimaterial notch has extensively been studied by many researchers in different applicable geometrical and material configurations [7–14]. In this field, Bogy [8, 9] and Hein and Erdogan [7] have formulated the stress and displacement fields of bimaterial corners and determined the order of stress singularity for different combinations of materials and corner angles. They indicated that both geometrical description and the elastic properties of the materials could strongly influence the state of singularity at the interface corners.

Despite the interest in research on the characteristic equation of bimaterial notch problem, the emphasis was put only on singular eigenvalues, while higher order eigenvalues have not been thoroughly studied. On the other hand, the recent investigations indicated that the higher order terms can significantly affect distribution of stress field adjacent a homogeneous and bimaterial notch tip [15–20]. Among these higher order terms, the first non-singular stress terms which are called V-stress in homogeneous notches and I-stress in bimaterial notches are the most effective terms, whereas disregard of these terms may result in a significant error in estimating the stress distribution near the corner [16, 20].

In this paper, a comprehensive study is done on characteristic equation of elastic stress field of bimaterial notches. In addition to singular eigenvalues, the eigenvalue associated with I-stress term is studied as well. The study is done on different combinations of materials and geometrical configuration. The combinations of materials were selected for two of the most applicable lines of the Body diagram, $\beta = \alpha/4$ and $\beta = 0$, for different values of α. The results indicate that both geometrical configuration and material combination significantly affect the order of singularity and the value of first non-singular eigenvalue. Finally, the area with high stress singularity between these two lines was determined and discussed.

1. **Characteristic Equation of Elastic Stress Field near a Bimaterial Notch Tip**. The asymptotic free-edge stress and displacement fields near a bimaterial notch tip can be obtained using Airy's stress function approach. Using this method, it can be indicated that the stresses and displacements near a bimaterial notch tip, shown in Fig. 1, subjected to a remote mechanical load can be represented as

$$\sigma_{ij}^{m} = \sum_{k=1}^{N} H_k r^{\lambda_k - 1} f_{ijk}^{m},$$
$$u_i^{m} = \sum_{k=1}^{N} H_k r^{\lambda_k} g_{ik}^{m}, \tag{1}$$

where $(i, j) \equiv (r, \theta)$ are the polar coordinates located at the bimaterial notch tip, $m = 1, 2$ represents the material number, and λ_k corresponds to the kth eigenvalue. Also in Eq. (1), f_{ijk} and g_{ik} are known functions of elastic properties of the materials, eigenvalues λ_k, the local geometry characterized by the angles θ_1 and θ_2, and the polar coordinate θ. The eigenvalues of a bimaterial problem are obtained by solving numerically the characteristic equation and they depend not only on the corner geometry characterized by θ_1 and θ_2 but also on the elastic properties of each material.

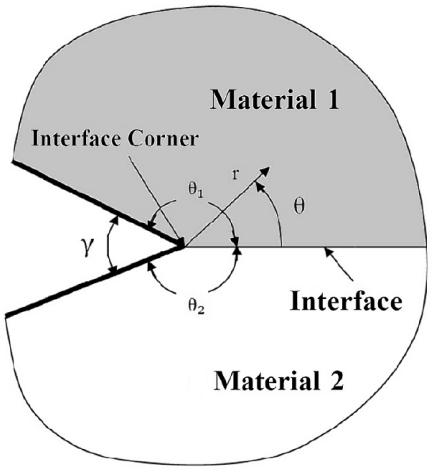

Fig. 1. General configuration of a bimaterial notch.

Due to the presence of stress term containing expression $r^{\lambda_k - 1}$, it is clear that the real eigenvalues in the range of $0 \le \lambda_k \le 1$ result in a stress singularity. The term $|\lambda_k - 1|$ which represents the intensity of the singularity near the interface corner is referred to as the order of singularity and it increases when λ_k approaches zero. There are one or two eigenvalues in the range of $0 \le \lambda_k \le 1$, depending on the combination of materials and geometrical configuration. There are also different numbers of higher order eigenvalues $\lambda_k \ge 1$ representing non-singular terms of stress field near the interface corner.

The eigenvalues λ_k can be extracted by solving the characteristic equation for the values of λ:

$$F = e^2 + b^2 - c^2 - d^2 = 0, \tag{2}$$

where

$$e = (\alpha - \beta)\{\cos(2\lambda\theta_1) - \cos(2\lambda\theta_1 - 2\lambda\theta_2) + \lambda^2[\cos(2\theta_1) - \cos(2\theta_1 + 2\theta_2) -$$

$$-1 + \cos(2\theta_2)]\} + (1+\alpha)[1 - \cos(2\lambda\theta_1)] - (1-\beta)[1 - \cos(2\lambda\theta_2)], \tag{3a}$$

$$b = (\alpha - \beta)\{\sin(2\lambda\theta_1) - \sin(2\lambda\theta_1 - 2\lambda\theta_2) - \lambda^2[\sin(2\theta_1) - \sin(2\theta_1 + 2\theta_2) +$$

$$+ \sin(2\theta_2)]\} - (1+\alpha)\sin(2\lambda\theta_1) - (1-\beta)\sin(2\lambda\theta_2), \tag{3b}$$

$$c = \lambda\{(\alpha - \beta)[\cos(2\lambda\theta_1) - \cos(2\lambda\theta_1 + 2\theta_2) + \cos(2\lambda\theta_2) - \cos(2\lambda\theta_2 - 2\theta_1) -$$

$$-1 + \cos(2\theta_1)] + (1+\alpha)[1 - \cos(2\theta_1)] - (1-\beta)[1 - \cos(2\theta_2)]\}, \tag{3c}$$

$$d = \lambda\{(\alpha - \beta)[\sin(2\theta_1) + \sin(2\lambda\theta_2 - 2\theta_1) - \sin(2\theta_1) + \sin(2\theta_1 + 2\theta_2) -$$

$$-\sin(2\lambda\theta_2)] - (1+\alpha)\sin(2\theta_1) - (1-\beta)\sin(2\theta_2)\}. \tag{3d}$$

The parameters α and β, called Dundurs' elastic mismatch parameters, are defined as

$$\alpha = \frac{\mu_1(\kappa_2+1)-\mu_2(\kappa_1+1)}{\mu_1(\kappa_2+1)+\mu_2(\kappa_1+1)}, \qquad \beta = \frac{\mu_1(\kappa_2-1)-\mu_2(\kappa_1-1)}{\mu_1(\kappa_2+1)+\mu_2(\kappa_1+1)}. \tag{4}$$

In this equation, E_m, ν_m, and $\mu_m = E_m/[2(1+\nu_m)]$ are the Young modulus, Poisson's ratio and shear modulus associated with the material m ($m=1, 2$), respectively. The parameter κ_m is equal to $3-4\nu_m$ for the plane strain and $(3-\nu_m)/(1+\nu_m)$ for the plane stress conditions. It can be seen when $\mu_1/\mu_2 \to \infty$ or $\mu_1/\mu_2 \to 0$, the parameter α approaches 1 or -1, respectively. On the other hand, by considering the restriction of $0 < \nu_m < 1/2$ and assuming the plane strain conditions, the parameter β varies only between $(\alpha+1)/4$ and $(\alpha-1)/4$ in terms of parameter α. For the plane strain condition, all the values of mismatch parameters α and β are contained within a parallelogram enclosed between $\alpha = \pm 1$ and $\alpha - 4\beta = \pm 1$ in the $\alpha - \beta$ plane. The point $\alpha = \beta = 0$ represents the condition associated with a homogeneous notch with identical materials. It is also noteworthy that the sign of α depends on the relative stiffness of materials 1 and 2.

The mismatch parameter α is positive when material 2 is more compliant than material 1, and negative when material 2 is stiffer than material 1. In this paper, the material 1 is considered to be stiffer than material 2, and thus the combinations of material can be selected from the first and fourth quadrants of $\alpha - \beta$ plane. On the other hand, Fig. 2 illustrates the values of mismatch parameters for some mostly-used combinations of material [16]. It can be seen that for a wide range of the bimaterial joints, the mismatch parameters are concentrated along and between lines $\beta = \alpha/4$ and $\beta = 0$ in the $\alpha - \beta$ space, with more data points near $\beta = \alpha/4$. Therefore, in the current paper the lines $\beta = \alpha/4$ and $\beta = 0$ are considered for study of the characteristic equation.

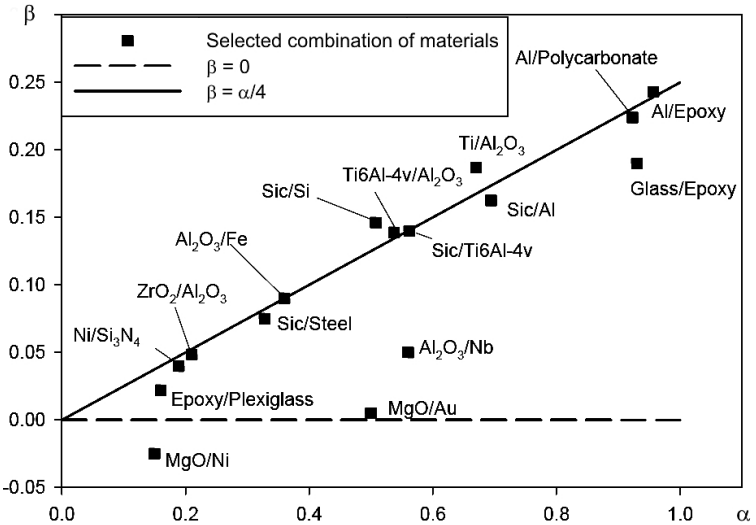

Fig. 2. Values of elastic mismatch parameters α and β in plane strain condition for selected combination of materials [16].

It should be noted that the angles θ_1 and θ_2 are assumed to be equal in this paper giving $\theta_1 = \theta_2 = \pi - (\gamma/2)$. Therefore, by considering different values of α in the range of $0 \le \alpha < 1$ and $\theta_1 = \theta_2 = \pi - (\gamma/2)$, the eigenvalues corresponding to both singular and first non-singular terms can be calculated by solving Eq. (2) numerically.

It is also noteworthy that the first singular eigenvalue represents the mode I (opening mode) and the second singular one is associated with the mode II (sliding mode) of the edge motion after applying the external load [3, 15].

2. **Results and Discussions**.

2.1. ***Singular Eigenvalues***. In this section, singular eigenvalues are studied as a function of opening angle γ and mismatch parameters α and β.

2.1.1. *First Singular Eigenvalue*. Figures 3 and 4 indicate the variation of the first singular eigenvalue corresponding to the mode I versus opening angle γ, across two lines $\beta = 0$ and $\beta = \alpha/4$. It can be seen that, in case of $\beta = 0$, the first singular eigenvalue increases with increasing opening angle γ and decreases with increasing mismatch parameter α for a constant value of γ. It also can be seen that for all opening angles and mismatch parameter α, the first singular eigenvalue is a real value.

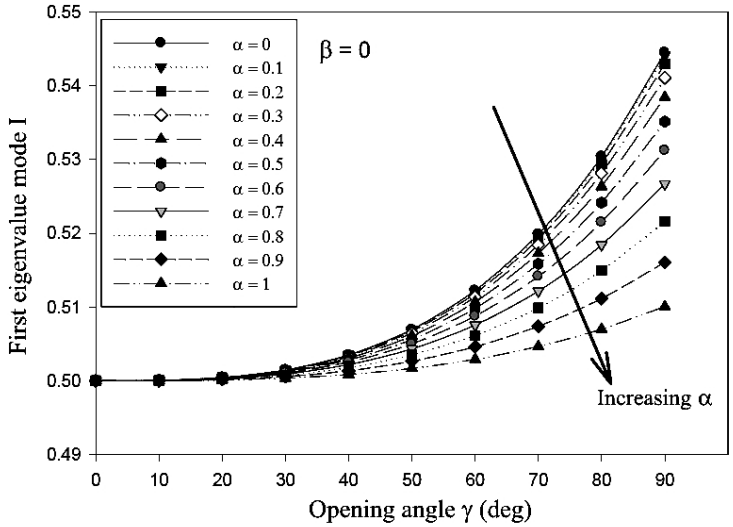

Fig. 3. Variation of first singular eigenvalue versus opening angle γ for $\beta = 0$.

In case of $\beta = \alpha/4$, the first singular eigenvalue has the imaginary part, as well as the real part when the opening angle is small. With increasing opening angle the imaginary part disappears, while the real part decreases with increasing opening angle. It should be noted that only real part is plotted in Fig. 4 as a function of opening angle. It is seen that the real part attains its maximum value at the point, where the imaginary part disappears. It also can be seen that the first singular eigenvalue increases with increasing α for a constant opening angle.

It should be mentioned that only real parts of the eigenvalues (singular and nonsingular) are studied in this paper. In fact, only real parts of the eigenvalues directly affect stress distribution near homogeneous and bimaterial notches. This is

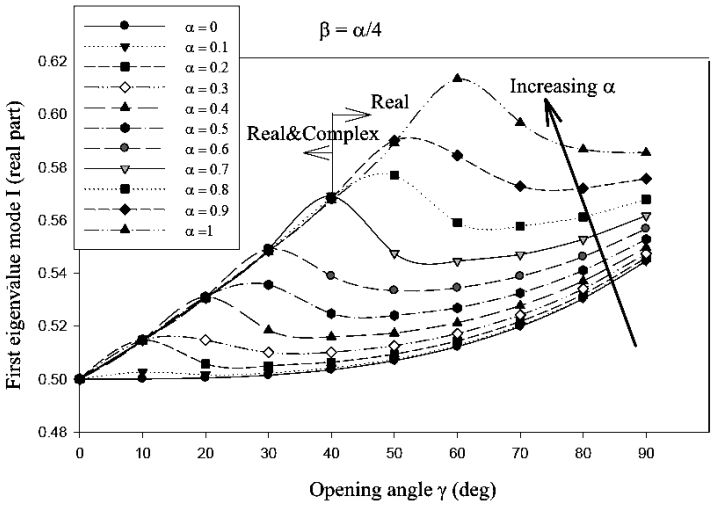

Fig. 4. Variation of real part of the first singular eigenvalue versus opening angle γ for $\beta = \alpha/4$.

because the complex eigenvalues of the notch problem (homogeneous or bimaterial) are conjugate and their effects counteract each other finally [15, 19].

2.1.2. *Second Singular Eigenvalue*. In Figs. 5 and 6, the variation of the second singular eigenvalue (associated with sliding mode) is illustrated as a function of opening angle γ, for $\beta = 0$ and $\beta = \alpha/4$. It can be seen that for $\beta = 0$, the second singular eigenvalue is always a real value and increases with increasing γ having a higher slope than the first singular eigenvalue (see Fig. 3). Also, second singular eigenvalue increases by increasing α for a constant value of γ. For $\beta = \alpha/4$, the second singular eigenvalue is a complex value which changes into a real value with increasing opening angle γ. In fact, for $\beta = \alpha/4$ the second singular eigenvalue is the conjugate value of the first singular eigenvalue in small values of γ. It also can be seen that for both $\beta = 0$ and $\beta = \alpha/4$, the real part of the second eigenvalue is increased with increasing opening angle γ.

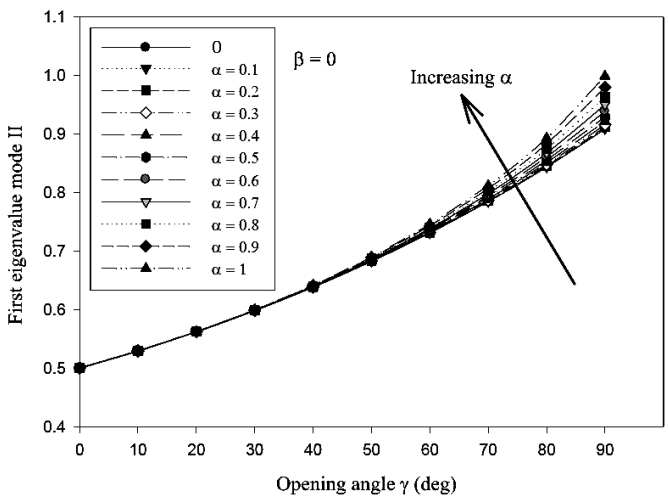

Fig. 5. Variation of second singular eigenvalue versus opening angle γ for $\beta = 0$.

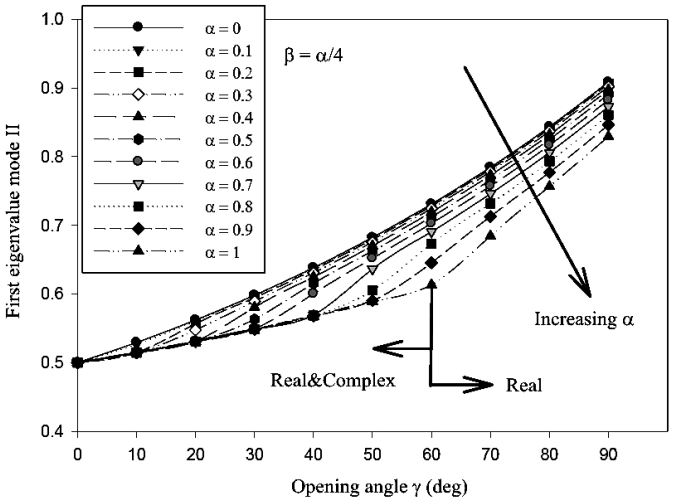

Fig. 6. Variation of real part of the second singular eigenvalue versus opening angle γ for $\beta = \alpha/4$.

2.2. ***First Non-Singular Eigenvalues***. As it was mentioned in the introduction, recent studies on the homogeneous and bimaterial notched specimens indicate that the first non-singular stress term can significantly influence on the stress distribution near the notch tip .Therefore, study of variation of the first non-singular eigenvalue as a function of opening angle and mismatch parameters is necessary. This section focuses on variation of this eigenvalue versus geometry and mismatch parameters in a wide range of opening angles and applicable combinations of materials.

Figures 7 and 8 show variation of the first non-singular eigenvalue as a function of γ for $\beta = 0$, $0 < \alpha < 1$ and $\beta = \alpha/4$, $0 < \alpha < 1$. It can be seen that for both cases, the eigenvalue is a real value at first and changes into a complex value by increasing the opening angle γ. In fact, by increasing the value of the opening angle, the first nonsingular eigenvalue chaotically changes from a real value to a complex value but the first transition does not occur at angles less than 44.9°.

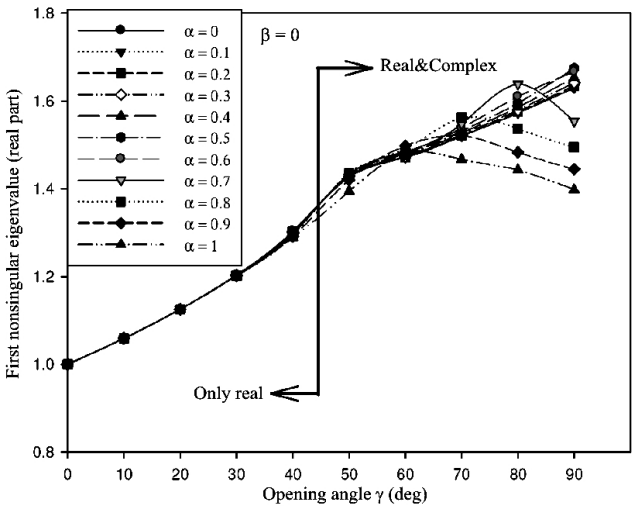

Fig. 7. Variation of real part of the first non-singular eigenvalue versus opening angle γ for $\beta = 0$.

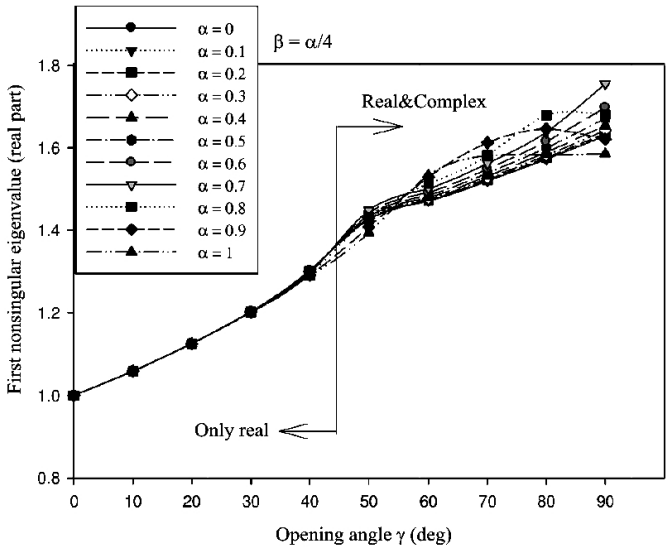

Fig. 8. Variation of real part of the first non-singular eigenvalue versus opening angle γ for $\beta = \alpha/4$.

The opening angle corresponding to the first transition from real to complex value which is called critical opening angle, γ_{cr}, is around 44.9° for homogeneous notches and varies in bimaterial notches for different values of α. In Fig. 9, the critical opening angle γ_{cr} is plotted as a function of mismatch parameter α. It is seen that at $\alpha = 0$ (associated with the homogeneous notches), the critical opening angle γ_{cr} is 44.9° and this value increases with increasing α. It also can be seen that for $\beta = \alpha/4$, value of γ_{cr} increases with a higher slope than that for $\beta = 0$.

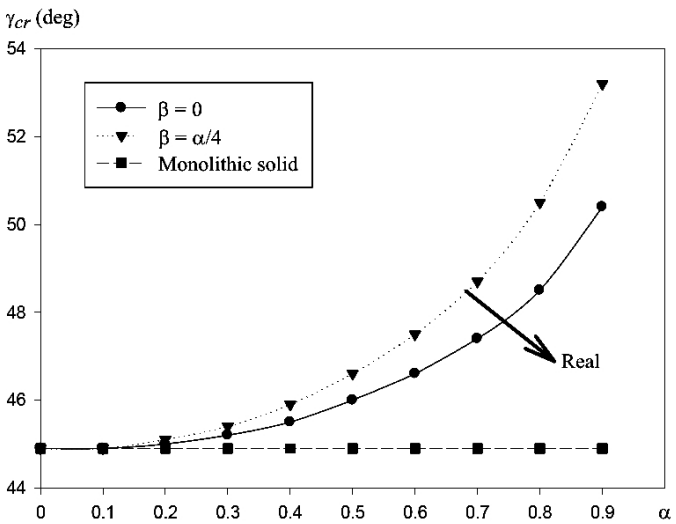

Fig. 9. Variation of critical opening angle for the first non-singular eigenvalue.

2.3. ***Areas with Higher Order of Singularity***. As it was mentioned in Section 1, the term $|\lambda_k - 1|$ is referred to as order of singularity, and it increases when λ_k approaches zero. In this section, the areas with higher order of singularity in the

Bogy diagram are determined for singular eigenvalues. The results plotted in Figs. 3–6 illustrated the variation of singular eigenvalues as a function of corner geometry and combination of materials.

In order to determine the high order of singularity areas, the range $0.5 < \lambda < 0.55$ for the first singular eigenvalue (eigenvalue of mode I) and $0.5 < \lambda < 0.7$ for the second singular eigenvalue (eigenvalue of mode II) are considered. Figure 10 indicates a limited area in the Bogy diagram between two lines $\beta = 0$ and $\beta = \alpha/4$ representing the first singular eigenvalue in the range of $0.5 < \lambda < 0.55$ and $0 < \gamma < 90°$. It is seen that for $\alpha > 0.6$ the first singular eigenvalue may fall outside the selected range.

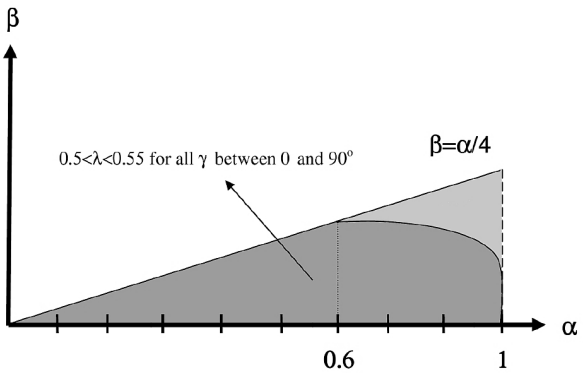

Fig. 10. Area with higher order of singularity for the first singular eigenvalue in the range of $0.5 < \lambda < 0.55$ and $0 < \gamma < 90°$ limited by $\beta = 0$ and $\beta = \alpha/4$.

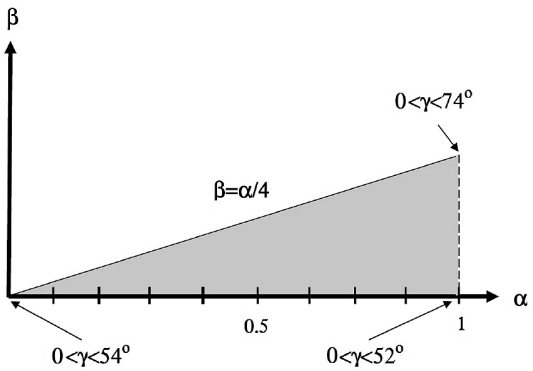

Fig. 11. Area with high order of singularity for the second singular eigenvalue in the range of $0.5 < \lambda < 0.7$ limited by the maximum opening angles.

Figure 11 shows the area in the Bogy diagram corresponding to the range of $0.5 < \lambda < 0.7$ for the second singular eigenvalue. It is seen that in this case, the restriction is on the opening angle γ. Therefore, the second singular eigenvalue is in the range of $0.5 < \lambda < 0.7$ for all values of mismatch parameters by considering the restriction in γ as shown in the corners of the shown area. For higher opening angle, the second singular eigenvalue falls outside the above-mentioned range.

It is clear from Figs. 10 and 11 that for first singular eigenvalue the order of singularity is sensitive of mismatch parameter α, while the second singular eigenvalue is sensitive to the opening angle γ.

Conclusions. The characteristic equation of elastic stress field near a bimaterial notch tip was studied. The analysis was done on the most applicable combination of materials and geometrical configurations in the Bogy diagram between lines $\beta = 0$ and $\beta = \alpha/4$. In addition to singular eigenvalues, the first nonsingular eigenvalue was also studied. For different combination of materials and geometrical configuration, singular and first nonsingular eigenvalues were comprehensively studied. Finally, the areas between lines $\beta = 0$ and $\beta = \alpha/4$ with more singularity were determined. It was shown that the first singular eigenvalue is sensitive of mismatch parameter α, while the second singular eigenvalue is sensitive to the opening angle γ. It also was shown that, in the case of $\beta = 0$, both the first and second singular eigenvalues are increased with increasing opening angle for the same combination of materials. However, the first singular eigenvalue decreases and the second singular eigenvalue increases with increasing α at the constant value of the opening angle. The results presented in this paper can be used for estimating the order of singularity as a function of combination of materials and corner geometry in the most applicable bonded joints.

Р е з ю м е

Досліджується характеристичне рівняння для пружного поля напружень у вістрі надрізу на стику двох матеріалів. Установлено, що руйнування відбувається в кутових точках їх стику через виникнення сингулярних напружень внаслідок розриву суцільності матеріалу й особливостей геометричної конфігурації. У полі пружних напружень у вістрі надрізу на стику двох матеріалів порядок такої сингулярності визначають власні значення функції напружень Ері. Проаналізовано сингулярні власні значення і маловивчене перше несингулярне власне значення. Розглянуто різні комбінації матеріалів і геометричних конфігурацій для двох найбільш використовуваних траєкторій на діаграмі Богі ($\beta = 0$, $\beta = \alpha/4$) та детально проаналізовано отримані результати. Показано, що геометричні конфігурації і комбінації матеріалів у вістрі надрізу суттєво впливають на сингулярність напружень поблизу кутових точок надрізу. Області з високою сингулярністю напружень виділено між лініями $\beta = 0$ і $\beta = \alpha/4$ на діаграмі Богі і проаналізовано як для першого, так і другого сингулярного власного значення.

1. A. R. Akisanya and N. A. Fleck, “Interfacial cracking from the free-edge of a long bi-material strip,” *Int. J. Solids Struct.*, **34**, 1645–1665 (1997).
2. A. R. Akisanya, “On the singular stress field near the edge of bonded joints,” *J. Strain Anal. Eng. Design*, **32**, 301–311 (1997).
3. M. L. Dunn, S. J. Cunningham, and P. E. W. Labossiere, “Initiation toughness of silicon/glass anodic bonds,” *Acta Mater.*, **48**, 735–744 (2000).
4. T. J. Lu, D. F. Moore, and M. H. Chia, “Mechanics of micromechanical clips for optical fibers,” *J. Micromech. Microeng.*, **12**, 168–176 (2002).
5. H. L. J. Pang, X. Zhang, X. Shi, and Z. P. Wang, “Interfacial fracture toughness test methodology for adhesive bonded joints,” *IEEE Trans. on Components and Packaging Technologies*, **25**, 187–191 (2002).

6. Y. Q. Yang, H. J. Dudek, and J. Kumpfert, "Interfacial reaction and stability of SCS–6SiC/Ti–25Al–10Nb–3V–1Mo composites," *Mater. Sci. Eng. A*, **246**, 213–220 (1998).
7. V. L. Hein and F. Erdogan, "Stress singularities in a two-material wedge," *Int. J. Fract. Mech.*, **7**, 317–330 (1971).
8. D. B. Bogy, "Two edge-bonded elastic wedges of different materials and wedge angles under surface traction," *J. Appl. Mech*., **38**, 377–386 (1971).
9. D. B. Bogy, "Edge-bonded dissimilar orthogonal elastic wedges under normal and shear loading," *J. Appl. Mech*., **35**, 460–466 (1968).
10. I. Mohammed and K. M. Liechti, "The effect of corner angles in bimaterial structures," *Int. J. Solids Struct.*, **38**, 4375–4394 (2001).
11. L. Marsavina, A. D. Nurse, L. Braescu, and E. M. Craciun, "Stress singularity of symmetric free-edge joints with elasto-plastic behavior," *Comput. Mater. Sci.*, **52**, 282–286 (2012).
12. Zh. Niu, D. Ge, C. Cheng, et al., "Evaluation of the stress singularities of plane V-notches in bonded dissimilar materials," *Appl. Math. Model*., **33**, 1776–1792 (2009).
13. A. Rahman and A. C. W. Lau, "Singular stress fields in interfacial notches of hybrid metal matrix composites," *Composites Part B: Engineering*, **29**, 763–768 (1998).
14. L. Y. Shang, Z. L. Zhang, and B. Skallerud, "Evaluation of fracture mechanics parameters for free edges in multi-layered structures with weak singularities," *Int. J. Solids Struct*., **46**, 1134–1148 (2009).
15. M. R. Ayatollahi, M. M. Mirsayar, and M. Dehghany, "Experimental determination of stress field parameters in bi-material notches using photoelasticity," *Mater. Des*., **32**, 4901–4908 (2011).
16. M. R. Ayatollahi, M. M. Mirsayar, and M. Nejati, "Evaluation of first non-singular stress term in bi-material notches," *Comput. Mater. Sci*., **50**, 752–760 (2010).
17. M. R. Ayatollahi, M. Dehghany, and M. M. Mirsayar, "A comprehensive photoelastic study for mode I sharp V-notches," *Eur. J. Mech. - A/Solids*, **37**, No. 1, 216–230 (2013), DOI: 10.1016/j.euromechsol.2012.07.001 (2012).
18. M. R. Ayatollahi and M. Nejati, "Experimental evaluation of stress field around the sharp notches using photoelasticity," *Mater. Des*., **32**, 561–569 (2011).
19. M. R. Ayatollahi, M. Dehghany, and M. Nejati, "Fracture analysis of V-notched components – effects of first non-singular stress term," *Int. J. Solids Struct*., **48**, 1579–1589 (2011).
20. J. K. Kim and S. B. Cho, "Effect of second non-singular term of mode I near the tip of a V-notched crack," *Fatigue Fract. Eng. Mater. Struct.*, **32**, 346–356 (2009).

Received 06. 11. 2012